

# Low Voltage Ride-Through Strategy using Voltage Amplitude Command Dynamic Calibration for VSG

Xin Ren, Binbin Wu

Henan Polytechnic University, Henan Key Laboratory of Intelligent Detection and Control of Coal Mine Equipment, Jiaozuo 454000, Henan, China

---

## Abstract

Overcurrent and power-angle instability will occur in the converter controlled by virtual synchronous generator (VSG), when the grid voltage drops rapidly, a low voltage ride-through (LVRT) strategy using voltage amplitude command dynamic calibration is proposed. When the grid voltage drops rapidly, the voltage amplitude of the converter port is used as the voltage command value of the VSG in a short time, making the inner voltage potential of VSG can respond to the grid voltage drops rapidly. In order to reduce the influence of large voltage fluctuation of converter port on dynamic calibration of voltage amplitude command, a sliding filter is designed to extract the voltage amplitude of the converter port; the selection principle of dynamic calibration voltage is analyzed, the constraints of VSG output current amplitude and power-angle stability are considered, VSG power command is designed based on phasor diagram analysis method under grid voltage drops. Simulation results verify the effectiveness of the proposed control strategy.

## Keywords

Virtual Synchronous Generator; Low Voltage Ride Through; Voltage Amplitude Command; Dynamic Calibration.

---

## 1. Introduction

With the increasing degree of electronic power system, the inertia and damping of the system are decreasing, so Virtual Synchronous Generator (VSG) technology has been paid more attention by scholars [1,2,3], The VSG technology increases the stability of the power system by introducing virtual inertia and damping to enable the converter to have the output characteristics of a synchronous generator [4,5]. However, the converter does not have the overload capacity of the traditional generator. When the voltage amplitude drops rapidly in the power system, the converter will produce output overcurrent, power Angle instability and other problems, and its safe operation is faced with challenges [6,7]. It is of great significance to improve the low voltage traversal ability of the VSG control converter to make it have friendly interaction with the grid during the rapid voltage sag in the power grid, which is of great significance for the safe operation of the power electronic power system. The current source converter resets the reference current during voltage sag, reduces the converter's output active power, and makes the converter safely complete the low voltage crossing [8]. Literature [9] designed appropriate parameters under current limiting to improve the transient stability of phase-locked loop in VSG in the system. Literature [10,11] combined VSG with traditional low voltage crossing strategy to keep the output of the two control modes consistent, and realized low voltage crossing by mode switching during voltage drop and recovery. Literature [12] limits the output power Angle of VSG after voltage drop to limit the deviation of the output power Angle of VSG. In literature [13], adaptive parameter design is started during the transient period to enhance the transient crossing ability of the converter. Literature [14] uses virtual resistance and current phasor limiting to suppress

VSG's output overcurrent when the grid voltage drops sharply, and reasonably adjusts power instructions to reduce the acceleration area of VSG under the grid voltage disturbance and thus improve its power Angle stability. Literature [15] optimizes the time and size of virtual reactance switching to limit the converter's output overcurrent during grid voltage sag.

In view of the safety problem of the transformer under the grid voltage sag, this paper intends to propose a control strategy based on the dynamic calibration of voltage amplitude command, so that the potential in VSG can quickly respond to the grid voltage and limit the output overcurrent of VSG when the grid voltage drops rapidly. The power command is designed based on the voltage amplitude of the converter port, so as to improve the power Angle stability of VSG. In this paper, the output overcurrent and power Angle instability of the virtual synchronous generator during the rapid voltage sag period are analyzed, and the low voltage crossing strategy based on the dynamic calibration of voltage amplitude instruction is presented and the simulation results are verified and analyzed.

## 2. VSG Control Principle

Figure 1 is the diagram of VSG grid-connected control[16].  $U_{dc}$  is DC voltage,  $i_{lx}$ ,  $u_{vx}$ ,  $i_{vx}$ ,  $e_{px}$ ,  $e_{gx}(x=a,b,c)$  is inductance current, converter port voltage namely VSG output voltage, current, point of common coupling (PCC) voltage and power grid voltage,  $R_f$ ,  $L_f$  and  $C_f$  are the equivalent resistance of filter inductance, filter inductance and filter capacitance,  $R_x$  and  $L_x$  are the equivalent resistance and inductance of grid-connected lines and isolation transformers,  $R_g$  and  $L_g$  are the equivalent resistance and inductance of power grid.  $\theta_{VSG}$  is active loop output phase angle;  $P_{ref}$  and  $P_e$  are active power instruction value and output value;  $P_m$  is prime mover output power;  $Q_{ref}$  and  $Q_e$  are reactive power instruction value and output value.  $U_0$  and  $U_{ref}$  are the command values of potential and voltage in VSG,  $\omega_0$  and  $\omega$  are the reference angular velocity and output angular velocity of VSG,  $J$  and  $D$  are the virtual moment of inertia and virtual damping,  $k_p$  and  $k_q$  are the active frequency adjustment coefficient and the reactive loop integration coefficient.

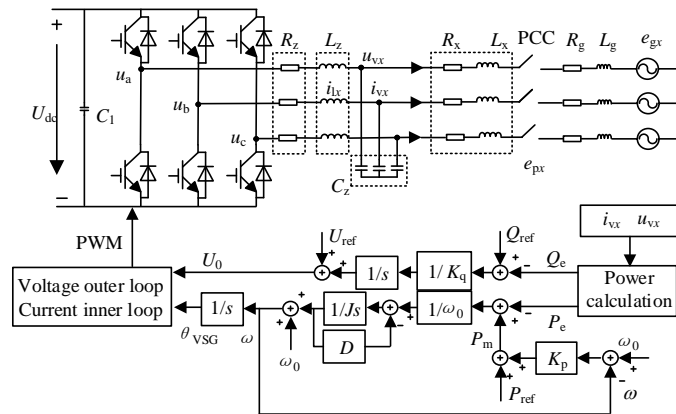


Figure 1. VSG grid-connected control diagram

According to figure 1, the governing equation of VSG active and reactive loops as shown in equations (1)(2).

$$\begin{cases} P_m = P_{ref} + k_p(\omega_0 - \omega_{VSG}) \\ J \frac{d^2 \theta_{VSG}}{dt^2} = \frac{P_m - P_e}{\omega_0} - D(\omega_{VSG} - \omega_0) \end{cases} \quad (1)$$

$$U_0 = (Q_{\text{ref}} - Q_e) \frac{1}{k_{qs}} + U_{\text{ref}} \quad (2)$$

Ignoring the line equivalent resistance, the power delivered by VSG to the grid is shown in equation (3)[17]:

$$\begin{cases} P_e = \frac{3 U_v E_p}{2 X_x} \sin \delta \\ Q_e = \frac{3 E_p}{2} \frac{E_p - U_v \cos \delta}{X_x} \end{cases} \quad (3)$$

$$X_x = \omega_0 L_x \quad (4)$$

In equations (3)(4):  $U_v$ ,  $E_p$  is the voltage amplitude of the converter port and the voltage amplitude of the junction point,  $\delta$  is the output power angle of VSG.

### 3. Analysis of Power Angle of VSG Output Current under Voltage Sag

#### 3.1 VSG Output Current Analysis

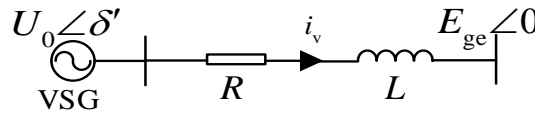


Figure 2. VSG grid-connected equivalent circuit

The equivalent circuit of VSG in grid-connected state is shown in figure 2,  $E_{ge}$  is the voltage amplitude behind the grid voltage drop,  $R=R_X+R_f+R_g$  and  $L=L_X+L_f+L_g$  are the line equivalent resistance and inductance,  $\delta'$  is the phase angle of  $U_0$  leading  $E_{ge}$ . When the grid voltage drops, the converter output current is;

$$i_v(t) = i_{ve}(t) + (i_0 - i_{ve0})e^{-\frac{t}{\tau}} \quad (5)$$

In equation (5):  $i_{ve}(t)$  is the steady-state current after voltage drop,  $i_0$  is the current value at the moment of voltage drop,  $i_{ve0}$  is the initial value of  $i_{ve}(t)$ ,  $\tau$  is the time attenuation constant.

When VSG voltage and power instructions do not change, the potential in VSG before and after grid voltage drop can be approximately regarded as unchanged,  $i_{ve}(t)$  is shown in equation (6).

$$i_{ve}(t) = \frac{U_0 \sin(\omega_0 t + \theta + \delta' - \varphi) - E_{ge} \sin(\omega_0 t + \theta - \varphi)}{\sqrt{R^2 + (j\omega_0 L)^2}} \quad (6)$$

In equation (6):  $\theta$  is the voltage phase of the grid,  $\varphi$  is the line impedance angle.  
Making  $t=0$ , the initial current values  $i_{ve0}$  and  $i_0$  as shown in equation (7)(8).

$$i_{ve0} = \frac{U_0 \sin(\theta + \delta' - \varphi) - E_{ge} \sin(\theta - \varphi)}{\sqrt{R^2 + (j\omega_0 L)^2}} \quad (7)$$

$$i_0 = \frac{U_0 \sin(\theta + \delta' - \varphi) - E_{ge} \sin(\theta - \varphi)}{\sqrt{R^2 + (j\omega_0 L)^2}} \quad (8)$$

As can be seen from equations (5)-(8), when the grid voltage falls, the potential  $U_0$  in VSG and the grid voltage  $E_{ge}$  produce a large vector difference, resulting in the converter's output current amplitude much larger than the normal state, and the greater the voltage sag depth, the greater the output current, the converter will face serious risk of overcurrent. Based on the above analysis, the output current of the converter can be reduced if the vector difference between potential  $U_0$  and grid voltage  $E_{ge}$  is reduced in VSG when the grid voltage sags.

### 3.2 VSG Output Power Angle analysis

As shown in figure 3(a), A cure is the power angle curve of VSG under normal condition, and VSG operates at the power angle  $\delta_A$  to output the specified active power  $P_{ref}$ . When the grid voltage sag is not deep, the power angle curve changes from A cure to B cure, and from A1 point to B1 points, the output angular velocity and power angle of VSG increase, accelerate the operation to B2 point, and gradually stabilize after  $\delta_B$  oscillations, reaching a new stable state. As shown in figure 3(b), when the grid voltage sag degree is deep, the power angle curve changes from A cure to C cure and from A1 point to C1 point.,the output power angle and output power of VSG gradually increase, and the output power cannot be equal to the power instruction value on the new power angle curve  $P_{ref}$ . According to the equal area theory, if the acceleration area during voltage sag is greater than the deceleration area after voltage recovery, VSG will have power angle instability.

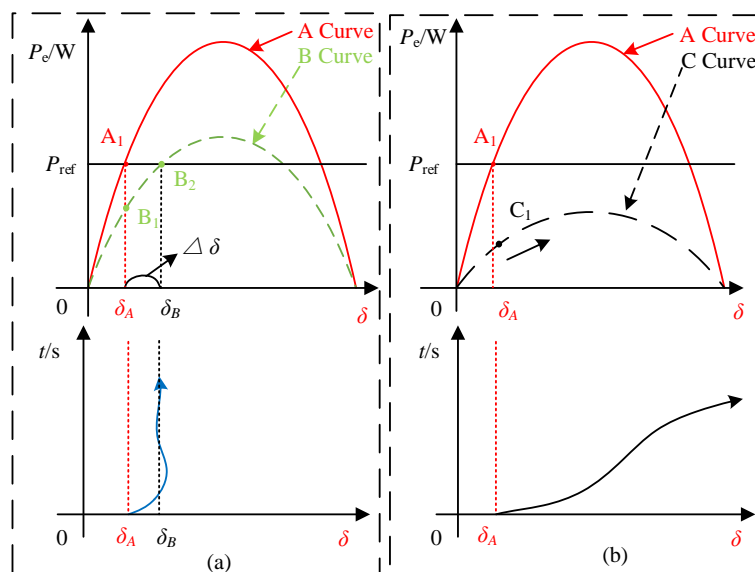


Figure 3. VSG output power angle curve

## 4. Low Voltage Ride-through Strategy Using Voltage Amplitude Command Dynamic Calibration

### 4.1 Voltage Amplitude Command Dynamic Calibration Method

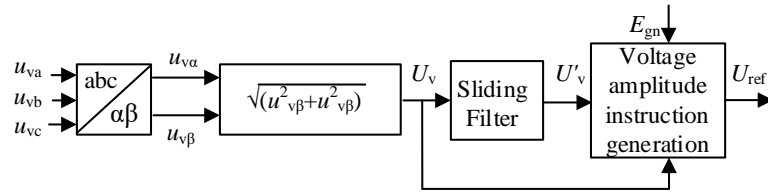


Figure 4. Block diagram of dynamic calibration method for voltage amplitude command

Figure 4 shows the block diagram of dynamic calibration method of voltage amplitude instruction, and  $u_{v\alpha}$  and  $u_{v\beta}$  are the  $\alpha\beta$ -axis components of voltage at the converter port,  $U'_v$  is the voltage output of port voltage amplitude  $U_v$  after sliding filtering. In case of voltage drop, the appropriate voltage amplitude instruction at different stages is conducive to reducing the vector difference between the potential and the grid voltage in VSG and reducing the risk of the converter output overcurrent. Next, the generation method design of voltage amplitude instruction will be presented.

### 4.2 Sliding Filter Design

Taking the voltage amplitude of the grid falling to 0.5pu when it is 0.3s as an example, the voltage amplitude change curve of the converter port is shown in curve 1 of figure 5. It can be seen from curve 1 that the port voltage amplitude fluctuates greatly. If this voltage is used as the calibration voltage, the port voltage fluctuation will be further aggravated. Therefore, the design of sliding filter is added, and its structural block diagram is shown in figure 6,  $N$  is the width of sliding filter window, when the sampling frequency is 10 kHz and  $N$  is 5, 10, 15 and 20 respectively, the output voltage waveform is shown in curves 2, 3, 4 and 5 in figure 5. As can be seen from figure 5, when  $N$  is large, the output voltage fluctuation is small, but the dynamic response is slow, when  $N$  is small, the output voltage fluctuates greatly. In conclusion, this paper take  $N$  for 10, 3 as shown in figure 5 curves.

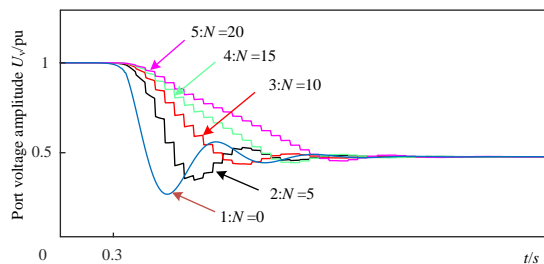


Figure 5. Port voltage amplitude  $U_v$  variation curve

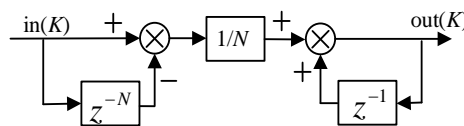
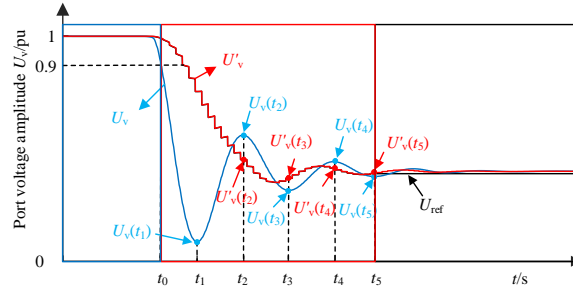


Figure 6. Block diagram of sliding filter

### 4.3 Voltage Amplitude Instruction Generation Method

Figure 7 shows the schematic diagram of the voltage amplitude command calibration.  $t_0$  is the moment when the port voltage amplitude is less than  $0.9E_{gn}$ , The  $U_v(t_y)$  ( $y=1,2,\dots$ ) is the extreme value of  $U_v$  voltage at time  $t_y$ , and  $U'_v(t_y)$  is the value of  $U'_v$  voltage at time  $t_y$ .



**Figure 7.** Voltage amplitude instruction calibration waveform diagram

Based on the grid voltage amplitude drop exceeding 10%, the generation method of voltage amplitude instruction follows the following steps and principles:

Step1: When  $U_v < 0.9E_{gn}$  is detected, set  $U_{ref} = U'_v$ ;

Step2: Record each extreme  $U_v(t_y)$  of the voltage drop  $U_v$ , and calculate the  $|U_v(t_y) - U_v(t_{y-1})| = \zeta(t_y)$ ;

Step3: Only when in  $t_y$  moment of  $\zeta(t_y) < 0.1U'_v(t_y)$ , if it is satisfied, let  $U_{ref} = U'_v(t_y)$  and keep  $U'_v(t_y)$  as the voltage amplitude command calibration value.

As shown in figure 7, if meet in  $t_5$  time  $|U_v(t_5) - U_v(t_4)| < 0.1U'_v(t_5)$ , according to the preceding steps, the voltage amplitude command is:

$$U_{ref} = \begin{cases} E_{gn} & 0.9E_{gn} \leq U_v \\ U'_v & t_0 < t \leq t_5 \& U_v < 0.9E_{gn} \\ U'_v(t_5) & t_5 < t \& U_v < 0.9E_{gn} \end{cases} \quad (9)$$

#### 4.4 Design of Power Command Adjustment Method

Figure8 shows the phasor relationship between system voltage and current when VSG is in stable operation.  $U_v$ ,  $E_p$  and  $U_x$  are the voltage phasor corresponding to the voltage across the impedance of  $U_v$ ,  $E_p$  and grid-connected lines, respectively,  $\alpha$ ,  $\beta$  and  $\varphi$  are respectively the included angle of  $U_v$  and  $I_v$ , the included angle of  $U_v$  and  $\Delta U$  and the impedance angle of grid-connected line  $Z_x = R_x + j\omega L_x$ .  $|U_x|$  amplitude,  $\alpha$ ,  $\beta$  and  $\varphi$ , respectively.

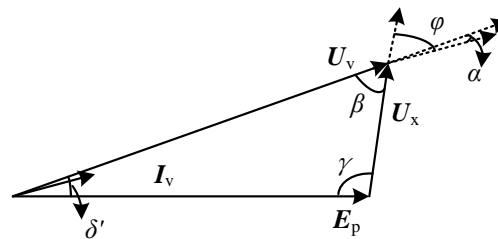


**Figure 8.** Phasor relation diagram of voltage and current in steady state

$$|U_x| = |Z_x| |I_v| \quad (10)$$

$$\varphi = \arctan \frac{\omega L_x}{R_x} \quad (11)$$

$$\alpha = \arccos\left(\frac{2P_e}{3|U_v||I_v|}\right) \quad (12)$$

$$\beta = \varphi - \alpha \quad (13)$$

The voltage amplitude and branch  $|E_p|$  and output power angle  $\delta$  of VSG under steady state operation can be expressed as equations (14)(15).

$$|E_p| = \sqrt{|U_x|^2 + |U_v|^2 - 2|U_x||U_v|\cos\beta} \quad (14)$$

$$\sin\delta = |U_x| \frac{\sin\beta}{|E_p|} \quad (15)$$

In order to keep VSG output power angle  $\delta$  and junction point stable after grid voltage drop, VSG output power Angle should be consistent with the power angle before the drop, at the same time, VSG can output enough reactive power to provide reactive support for the grid voltage, and the voltage drop behind the VSG output current amplitude to maintain its rated current amplitude, VSG power command value needs to be adjusted. The following will give the design method of the power instruction value satisfying the above conditions.

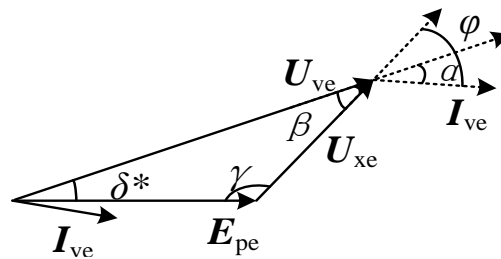


**Figure 9.** Phasor relation diagram of voltage and current with power command value adjustment

When the power grid voltage falls, the voltage and current phasor relationship adjusted by the new power command value is shown in figure9. In figure9,  $U_{ve}$ ,  $I_{ve}$ ,  $E_{pe}$  and  $U_{xe}$  are the voltage phasor at converter port, output current phasor, voltage phasor at connecting point, and voltage phasor at both ends of the grid-connected line, respectively.  $|I_{ve}|$  for VSG output rated current amplitude. Available in figure9 VSG output angle  $\delta^*$ , current amplitude  $|I_{ve}|$  and voltage amplitude  $|U_{xe}|$  as shown in equations (16)(17)(18).

$$\delta^* = \delta \quad (16)$$

$$|I_{ve}| = |I_v| \quad (17)$$

$$|U_{xe}| = |Z_x| |I_{ve}| \quad (18)$$

In combination with figure9, equations (16), (17) and (18) can be obtained:

$$\gamma = \arcsin \left( |U_{ve}| \frac{\sin \delta^*}{|U_{xe}|} \right) \quad (19)$$

$$\alpha = \varphi - (\pi - \delta^* - \gamma) \quad (20)$$

The active power  $P_e$  and reactive power  $Q_e$  output by VSG after the grid voltage falls are shown in equations (21)(22):

$$P_e = \frac{3}{2} |U_{ve}| |I_{ve}| \cos \alpha \quad (21)$$

$$Q_e = \frac{3}{2} |U_{ve}| |I_{ve}| \sin \alpha \quad (22)$$

## 5. Simulation Results and Analysis

Based on the parameters in figure 1 and table 1, a simulation model of the VSG controlled converter connected to the grid was built in MATLAB/Simulink, the rated value was taken as the reference value and the grid voltage dropped to 0.5pu was taken as an example. VSG operates in a stable state before voltage drop, voltage drop is detected at 0.3s and voltage recovery at 0.7s, compare and analyze the low voltage crossing effect of VSG in the conventional control strategy and the control strategy in this paper. the conventional control strategy does not add special control for low voltage crossing.

**Table 1.** Parameters of simulation

Parameter name	value	Parameter name	value
Dc bus voltage $U_{dc}/V$	800	Rated amplitude of power grid voltage $E_{gn}/V$	311
Filter resistance $R_f/\Omega$	0.2	Virtual inertia $J/kg \cdot m^2$	0.8
Filter inductance $L_f/mH$	1.5	Damping coefficient $D/N \cdot m \cdot s/rad$	40
Filter capacitance $C_f/mF$	0.03	Reactive droop coefficient $k_q$	0.3
Line resistance $R_x/\Omega$	0.5	Active droop coefficient $k_p$	1591.5
Line inductance $L_x/mH$	2	Carrier frequency $f/Hz$	10000
Rated active power $P/kW$	10	Rated reactive power $Q/var$	0

### 5.1 VSG Output Characteristics under Normal Control

The analysis of grid voltage waveform, VSG output voltage, current, power, power angle and output current THD under conventional control is shown in figure 10.



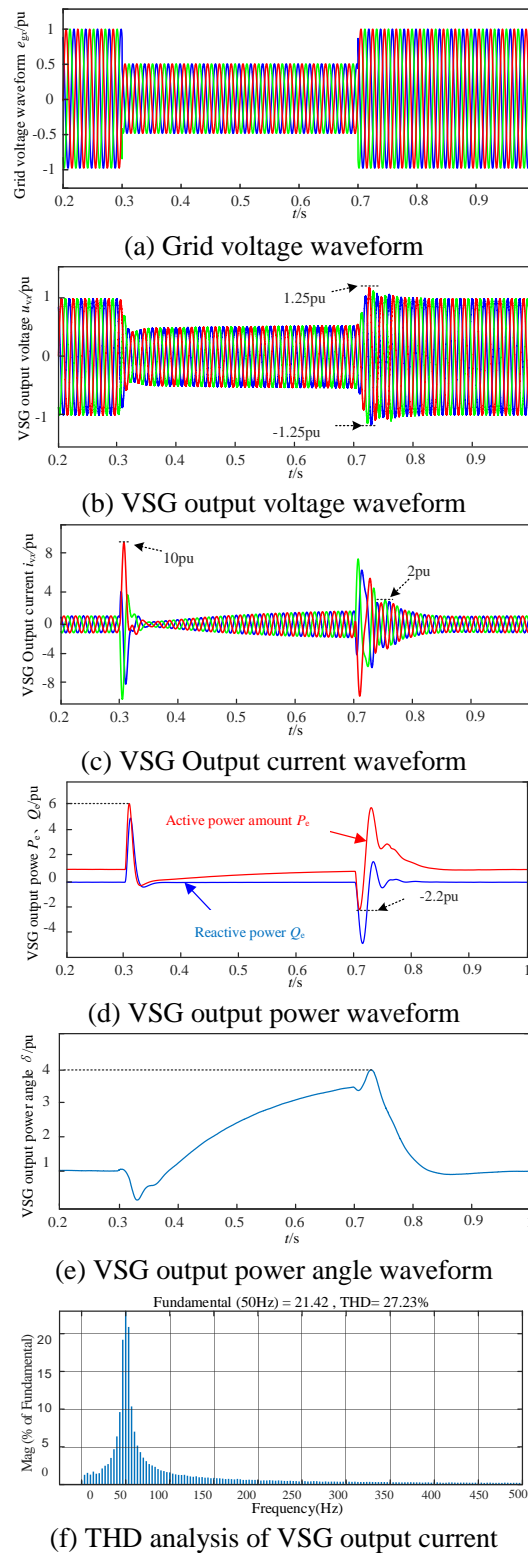
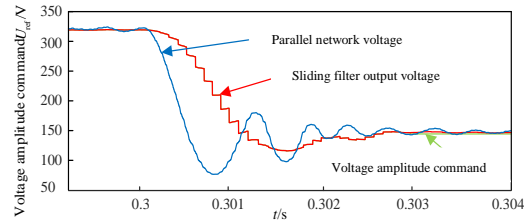


**Figure 10.** Simulation output waveform of VSG under symmetrical drop of grid voltage

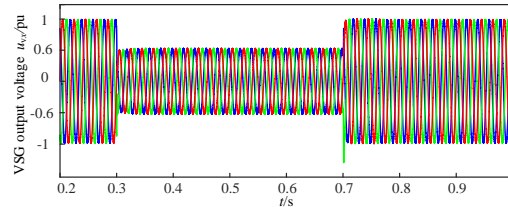
The grid voltage drops from 0.3s to 0.5pu, as shown in figure 10(b) and (c), during voltage sag, there is a large amplitude difference between the output voltage amplitude of VSG and that of the power grid, which makes the output current increase sharply. The maximum instantaneous value is 10pu, and the output overcurrent lasts a long time. As can be seen from figure (d), VSG's output power fluctuates greatly, and the maximum output active power and reactive power are 6pu and 5.5pu. As

can be seen from figure (e) and (f), the output power Angle of VSG increases continuously, up to 4 times of the rated value, the output current THD value is 27.23%, and the output current quality does not meet the requirements of grid-connection. It can be seen that VSG output current exceeds the converter's safety threshold for a long time, the power Angle keeps increasing, and the grid-connected power quality does not meet the grid-connected requirements, which seriously threatens the converter's safe operation and further reduces the power quality of the grid.

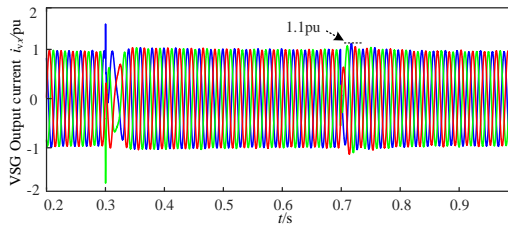
**5.2 This Article Traverses the VSG Output Feature of the Strategy**



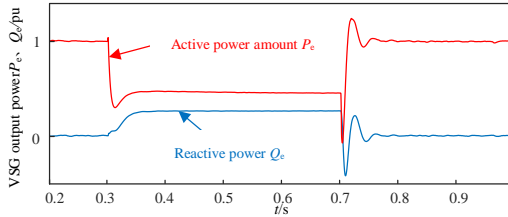
(a) Voltage amplitude command waveform



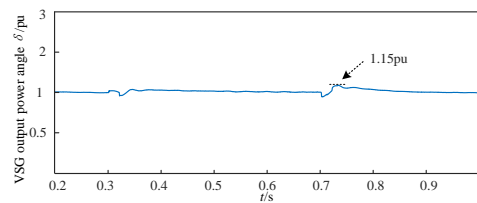
(b) VSG output voltage waveform



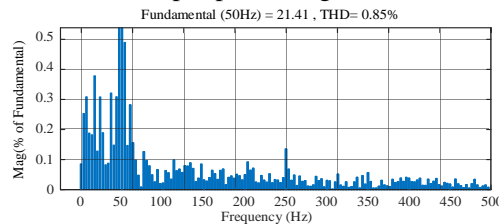
(c) VSG Output current waveform



(d) VSG output power waveform



(e) VSG output power angle waveform



(f) THD analysis of VSG output current

**Figure 11.** VSG simulation waveforms under voltage amplitude command calibration

After using the low voltage ride-through strategy using voltage amplitude command dynamic calibration, VSG simulation output waveform is shown in figure 11.

By comparing figure 10(a) and (b), it can be seen from figure 11(a) and (b) that: using the control strategy proposed in this paper, the voltage amplitude instruction 1 is calibrated after about 0.003s, and the output voltage of VSG can quickly follow the voltage drop of the grid. As can be seen from figure (c), VSG output current decreases below 2pu at the moment of voltage drop and recovery, and the duration is less than 0.001s, meanwhile, combined with figure (f), it can be seen that the output current amplitude of VSG is 21.78A, and the waveform distortion rate is about 1.6%, which meets the quality requirements of grid-connected current. According to the design of VSG power command adjustment method, when the grid voltage amplitude drop depth is 0.5pu, the theoretical output active power and reactive power are 4.7kW and 2.6kvar respectively, in figure (d), the output active and reactive power of VSG are 4.8kW and 2.64kvar respectively, and the error is 2% and 1.5% respectively compared with the theoretical analysis, the simulation results meet the theoretical analysis. As can be seen from figure (e), the output power angle of VSG fluctuates slightly during voltage drop and recovery, and the maximum power angle fluctuation is 1.1pu, the fluctuation of power angle is effectively improved, which keeps the output power angle of VSG stable during voltage sag, and helps to improve the speed of VSG recovering to the normal state before voltage sag after voltage recovery.

## 6. Conclusion

In order to improve the low voltage traversal ability of VSG, this paper analyzes the output current and power angle characteristics of VSG during rapid grid voltage drop, proposes a low voltage ride through strategy using voltage amplitude command dynamic calibration, and carries out simulation analysis. The research and simulation results show that: 1) The VSG voltage amplitude command dynamic calibration strategy was used to quickly calibrate the potential in the VSG, during the period of low voltage pass through, the VSG output impact current size was controlled below 2pu, and the duration was shortened to less than 0.001s, which effectively solved the problem of excessive impact current; 2) Through the adjustment of power instruction, the purpose of keeping the output power angle of VSG stable and the output current within the rated range in the process of low voltage crossing is achieved, and the output current quality meets the requirements of grid-connection. On the other hand, this paper is to improve VSG low voltage crossing capability from the perspective of VSG voltage amplitude instruction calibration, the effective combination of this method with virtual impedance and other methods needs further study.

## References

- [1] Lü Zhipeng, Sheng Wanxing, Zhong Qingchang, et al. Virtual synchronous generator and its applications in micro-grid[J]. Proceedings of the CSEE, 2014, 34(16): 2591-2603(in Chinese).
- [2] Zhong Q C, Weiss G. Synchronverters inverters that mimic synchronous generators[J]. IEEE Transactions on Industrial Electronics, 2011, 58(4): 1259-1267.
- [3] Hirase Y, Abe K, Sugimoto K, et al. A grid connected Inverter with virtual synchronous generator model of algebraic type[J]. IEEE Transactions on Power and Energy, 2011, 132: 371-380.
- [4] Zhang Yu, Cai Xu, Zhang Chen, et al. Transient synchronization stability analysis of voltage source converters: a review[J]. Proceedings of the CSEE, 2021, 41(05): 1687-1702(in Chinese).
- [5] ARGHIR C, JOUINI T, DÖRFLER F. Grid-forming control for power converters based on matching of synchronous machines[J]. Automatica, 2018, 95: 273-282.
- [6] Cheema K M, Milyani A H, El-Sherbeeney A M, et al. Modification in active power-frequency loop of virtual synchronous generator to improve the transient stability[J]. International Journal of Electrical Power & Energy Systems, 2021, 128: 106668.

- [7] HUANG L B, XIN H H, WANG Z. et al. Transient stability analysis and control design of droop-controlled voltage source converters considering current limitation [J]. IEEE Transactions on Smart Grid, 2019, 10(1):578-591.
- [8] Chen Yaai, Liu Jingdong, Zhou Jinghua. et al. Fault ride-through control strategy for solar grid-connected inverters[J]. Proceedings of the CSEE, 2014, 34(21): 3405-3412(in Chinese).
- [9] WU H, WANG X F. Transient stability impact of the phase-locked loop on grid-connected voltage source converters [C]//2018 International Power Electronics Conference (IPEC-Niigata 2018 -ECCE Asia), May 20-24, 2018, Niigata, Japan: 2673-2680.
- [10] Li Hua, Gao Huaizheng, Hao Yue, et al. Seamless switching control strategy for low voltage ride-through based on virtual synchronous generator[J]. Acta Energiæ Solaris Sinica, 2021, 42(03): 114-120(in Chinese).
- [11] Alipoor J, Miura Y, Ise T. Voltage sag ride-through performance of virtual synchronous generator[J]. IEEJ Journal of Industry Applications, 2015, 4(5): 654-666.
- [12] Fang Zhixue, Su Jianhui, Wang Huafeng, et al. Low voltage ride-through control strategy of microgrid inverter[J]. Automation of Electric Power Systems, 2019, 43(2): 143-149, 161(in Chinese).
- [13] HUANG L B, XIN H H, WANG Z, et al. An adaptive phase-locked loop to improve stability of voltage source converters in weak grids [C]//2018 IEEE Power & Energy Society General Meeting (PESGM), August 5-10, 2018, Portland, USA: 1-5.
- [14] Sun Jiahang, Feng Zhongnan, Huang Jingguang, et al. Low-voltage ride-through control strategy of wind-storage co-generation system based on improved VSG[J/OL]. Power System Technology, 1-14[2022-09-26]. DOI: 10.13335/j.1000-3673.pst.2022.0717(in Chinese).
- [15] Wang Xuemei, Wang Yibo, L Liu Yutong, et al. Low voltage ride through control method of actively supported new energy unit based on virtual reactance[J/OL]. Power System Technology, 1-11[2022-09-29]DOI: 10.13335/j.1000-3673.pst.2021.2148(in Chinese).
- [16] SUN Jie, YIN Taiyuan , WANG Yue, et al. Impedance modeling and grid-connected stability analysis of MMC under VSG control strategy[J]. Journal of Power Supply 2021, 19(06):30-41. DOI:10.13234/j.issn.2095-2805.2021.6.30.
- [17] LI Ming , ZHANG Xing, ZHANG Hang, et al, Modeling and analysis of VSG Output impedance and small-signal based on virtual steady-state synchronous impedance[J]. Journal of Power Supply, 2018, 16(06):11-17. DOI:10.13234/j.issn.2095-2805.2018.6.11.